J Electr Eng Technol Vol. 9, No. 5: 1623-1631, 2014
http://dx.doi.org/10.5370/JEET.2014.9.5.1623

ISSN(Print) 1975-0102
ISSN(Online) 2093-7423

Inductances Evaluation of a Squirrel-Cage Induction Motor with Curved Dynamic Eccentricity

Qiang Lv*, Xiaohua Bao†, Yigang He*, Yong Fang* and Xiaowei Cheng*

Abstract – Eccentricity faults more or less exist in all rotating electrical machines. This paper establishes a more precise model of dynamic eccentricity (DE) in electrical machines named as curved dynamic eccentricity. It is a kind of axial unequal eccentricity which has not been investigated in detail so far but occurs in large electrical machines. The inductances of a large three-phase squirrel-cage induction machine (SCIM) under different levels of curved DE conditions are evaluated using winding function approach (WFA). These inductances include the stator self and mutual inductances, rotor self and mutual inductances, and mutual inductances between stator phases and rotor loops. A comparison is made between the calculation results under curved DE and the corresponding pure DE conditions. It indicates that the eccentricity condition will be more terrible than the monitored eccentricity based on the conventional pure DE model.

Keywords: Curved dynamic eccentricity, Inductance evaluation, Induction machine, Winding function approach

1. Introduction

Rotating electrical machines are widely used in industrial processes, water conservancy, defense equipments, mining, etc. Due to the significant economic losses or emergencies caused by the sudden breakdown of electrical machines, fault diagnosis and condition monitoring are gaining more attention. Mechanical faults are common in electrical machines, and represent up to 50%~60% of the faults. Bearing faults and eccentricity between the stator and the rotor are among the critical and severe faults [1, 2]. Thus, an effective, accurate and quick method of evaluating eccentricity-related faults is of great importance.

Much effort has been made to investigate the performance of a machine with eccentricity so far. Briefly, eccentricity in rotating electrical machines is a condition that the air gap between the rotor and stator is not equal. This is caused by a lot of factors such as manufacture or installation tolerance, bearing wear, bent rotor shaft, load and so on. Air gap eccentricity in rotating electrical machines actually can not be avoided. The effects of interest caused by air gap eccentricity in a SCIM mainly include winding current harmonics, inductance, air-gap flux, unbalanced magnetic pull (UMP) between the rotor and stator, vibration, increased losses, torque variation, etc. Static eccentricity (SE) and dynamic eccentricity (DE) are introduced to basically describe the eccentricity. The multi-loop model is widely used in fault diagnosis and condition monitoring of electrical machines. Inductances evaluation as a critical part of the analytic method has drawn a lot of attention to researchers. Previous researches such as analysis and control of synchronous machines done by Lipo [3] provided a general expression of inductances between any two windings in an electrical machine, assuming that permeance of iron is infinite. Then Luo et al [4] presented a new multiple coupled circuit model for induction machines with both arbitrary winding layout and / or unbalanced operating conditions. An equation for calculating inductances based on the coil geometry was derived from winding function theory. And a good agreement with the solution obtained by a conventional *d-q* model was shown. Toliyat et al [5] proposed a method which enables the dynamic simulation of air gap eccentricity in induction machines. Inductances under static eccentricity were calculated using winding function method concerning MMF drop across the iron. Effects of stator and rotor slots were not included. Based on winding function approach, Joksimović et al [6] described a method for dynamic simulation of dynamic rotor eccentricity in SCIMs. The inverse air gap function was given by an approximate expression. Nandi et al [7] modeled the SCIM under mixed eccentricity condition using modified winding function approach (MWFA). And Faiz et al [8] gave a more precise model for computation of three-phase SCIM inductances under different eccentric conditions, including SE, DE and mixed eccentricity. This leads to an improved performance prediction of induction motor. Faiz et al also calculated the stator inductances considering the saturation effect in [9]. Later, Li et al [10] investigated the performance of a three-phase induction machine with nonuniform SE along axial direction or

† Corresponding Author: School of Electrical Engineering and Automation, Hefei University of Technology, P.R. China. (sukz@ustc.edu)
* School of Electrical Engineering and Automation, Hefei University of Technology, P.R. China. (lvqsz@mail.hfut.edu.cn, hyghnu@yahoo.com.cn, {rtrmoonsky, chengxiao_w}@163.com)
Received: June 17, 2013; Accepted: May 7, 2014

inclined SE. A variant of MWFA was applied to calculating the inductances. The effect of skew rotor bars is incorporated in the inductances calculation. The values of inductances were verified using finite element method. It showed that inclined eccentricity symmetric to the midpoint of the machine shaft could not be recognized from the current spectrum and would therefore require some other form of detection. Other kinds of axial-varying eccentricity mentioned in some papers are similar to the inclined eccentricity, such as simultaneous static air gap eccentricity and rotor misalignment fault studied in [11] and [12], eccentricity at one end only mentioned in [13].

However, the real air gap eccentricity of a rotating electrical machine is quite complicated. It is a combination of both SE and DE. Worse still, the degree of SE and DE usually varies along the axial direction. It can not be simply described as mixed eccentricity or inclined eccentricity. Fig. 1 (a) shows a 12-pole, three-phase, 2800-kW, 10-kV, 50-Hz submersible induction motor with rub-impact fault. From the inner surface of the stator, it can be seen that the rubbed area lies only in the middle part of the stator. In the case of large submersible motors used in mine pumps, this phenomenon would be more visible due to the slender structure if there is a stator-rotor contact. Apparently, only bent rotor would lead to the grinding crack shown in Fig. 1 (a). In addition, the unequal length of l_u and l_d indicates that inclined static eccentricity exists in the machine. Fig. 1 (b) illustrates the rub-impact fault of the electrical machine. Consequently, an axial unequal eccentricity named as curved dynamic eccentricity is proposed in this paper. This kind of eccentricity mainly occurs in large electrical machines with relatively long stack length, such as water filling submersible induction motors.

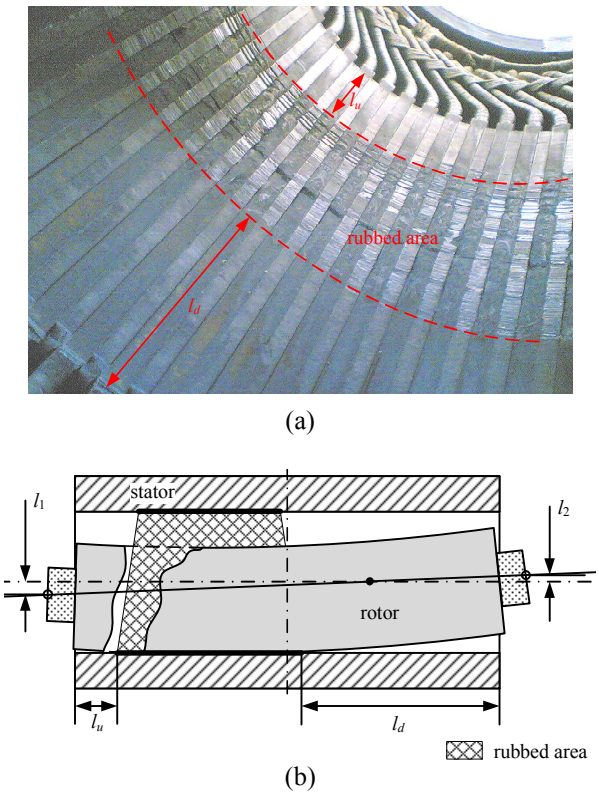

Fig. 1. (a) Stator inner surface of a three-phase submersible induction motor with rub-impact fault; (b) Illustration of the rub-impact fault

From the previous research mentioned above, it can be concluded that the multi-loop model is a fantastic way to theoretically solve the eccentricity related problems. The calculation of inductance matrixes in the multi-loop model is the key to the successful analysis, and has a great influence on the calculation results. So the authors devoted themselves to the calculation of inductances. Since the air-gap eccentricity has a remarkable impact on the value of inductances, the effect of curved DE is involved in the calculation. This paper evaluated the inductances of a three-phase SCIM with curved DE and analyzed the features of the curved DE. Due to the similarity between the curved DE and pure DE (dynamic eccentricity without axial variation) conditions, a comparison is made between these two conditions. It is shown that there is a certain level of pure DE condition under which the variation curves of inductances are quite close to the calculation results under the corresponding curved DE condition. This will lead to a significant error which can not be ignored during the estimation of DE using motor current signature analysis, because the certain level of pure DE is always less than the maximum eccentricity of the corresponding curved DE.

2. Modeling of Curved Dynamic Eccentricity

In the case of curved DE, the air-gap length changes in both radial and axial directions. Fig. 2 illustrates the model of curved DE. In order to highlight the features that are different from other kinds of eccentricity, this model is simplified from Fig.1 (b). The following are assumed in this model:

1) Static eccentricity or rotor misalignment does not exist in the machine;
2) The rotor core is bent, and the center of the shaft cross section is parabola-shaped;
3) The motor with curved DE is bilateral symmetrical.
4) The air-gap length of an electrical machine is defined by

$$g = r_{i1} - r_{o2} \tag{1}$$

where r_{i1} is the stator inner radius, and r_{o2} is the rotor outer radius. An accurate enough way of describing the air-gap length of a motor with DE is

$$g_d(y,t) = g_0\left[1 - \delta_d \cos\left(\omega_r t - y/r_a\right)\right] \tag{2}$$

where g_0 is the radial air-gap length when the rotor is centered, δ_d is the degree of eccentricity which is relative to g_0, ω_r is the rotational velocity in radians per second, t is time, y is the circumferential distance from a reference point, and r_a is the average air-gap radius. This function is widely used in a lot of papers [13-16].

When the rotor exhibits curved DE as Fig. 2 shows, the air-gap length can be expressed as

$$g_{cd}(x,y,t) = g_0\left[1-\delta_{cd}(x)\cos\left(\omega_r t - y/r_a\right)\right] \tag{3}$$

where $\delta_{cd}(x)$ is the degree of eccentricity, and it is a function of axial position x. For a motor under δ_{min} = 6% and δ_{max} = 25% curved DE condition, the degree of eccentricity can be fitted by a parabola:

$$\delta_{cd}(x) = -0.378698x^2 + 0.530178x + 0.0644378 \tag{4}$$

The rotational velocity in a three-phase induction motor is

$$\omega_r = \frac{2\pi f_s}{p}(1-s) \tag{5}$$

where f_s is the fundamental frequency of stator supply in Hertz, p is the pole pairs, and s is the slip.

The stator position φ measured from a reference point on the stator, and the rotor position θ measured from the same reference point can be expressed as follows:

$$\mathrm{j} = y/r_a \tag{6}$$

$$\theta = \omega_r t \tag{7}$$

If considering the starting process, the function of rotor position should be replaced by

$$\theta = \int_0^t \omega_r(t)\,dt \tag{8}$$

Therefore, Eq. (3) can be rewritten as

$$g_{cd}(x,\mathrm{j},\theta) = g_0\left[1-\delta_{cd}(x)\cos\left(\theta-\mathrm{j}\right)\right] \tag{9}$$

Then the inverse air-gap function can be defined as

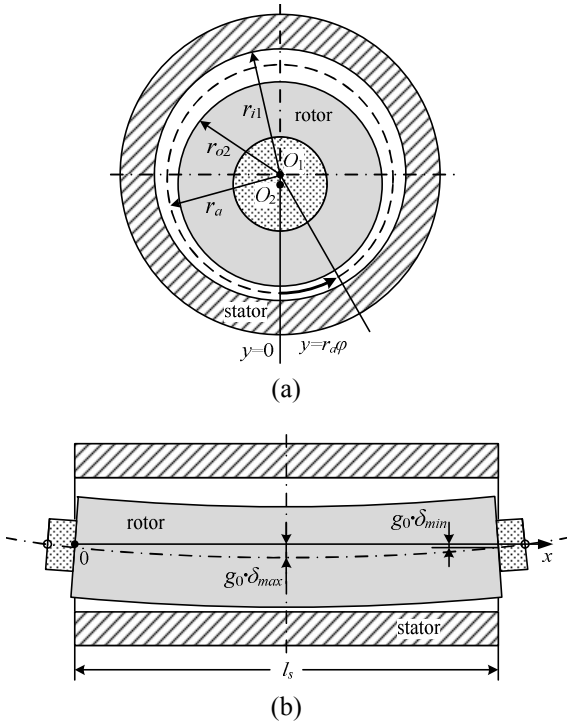

Fig. 2. (a) Circumferential unequal air gap. O_1 is the centre of the stator core. O_2 is the centre of the rotor core. (b) Axial curved unequal air gap. $g_0{\cdot}\delta_{max}$ is the maximum eccentricity. $g_0{\cdot}\delta_{min}$ is the minimum eccentricity.

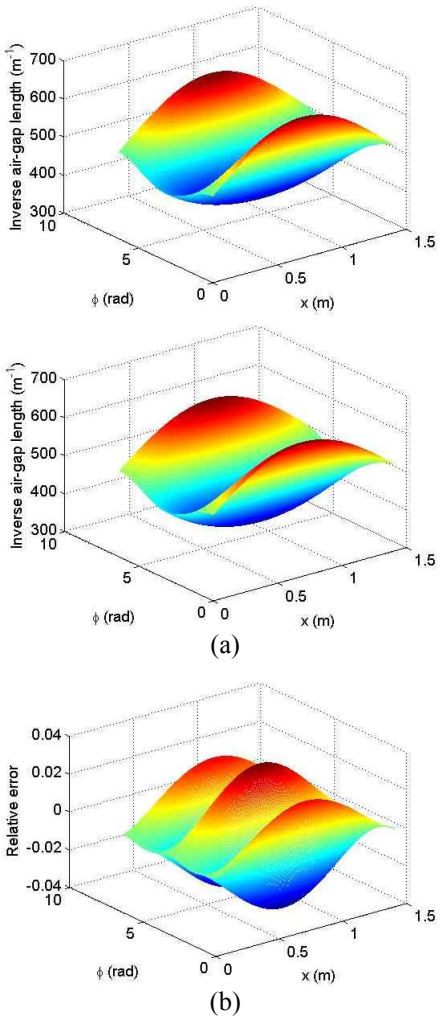

Fig. 3. (a) Precise (left) and approximate (right) inverse air-gap fluctuation at the initial position, for the δ_{min} =6% and δ_{max}=25% curved DE condition. (b) Relative error of the approximate inverse air-gap function.

$$g_{cd}^{-1}(x,\mathrm{j},\theta)=\frac{1}{g_0\left[1-\delta_{cd}(x)\cos(\theta-\mathrm{j})\right]} \tag{10}$$

With Fourier series analysis, and taking into account the first harmonic, the inverse air-gap function is given approximately as [5, 7-8]

$$g_{cd}^{-1}(x,\mathrm{j},\theta)\approx\frac{1}{g_0\sqrt{1-[\delta_{cd}(x)]^2}}+\frac{2}{g_0\sqrt{1-[\delta_{cd}(x)]^2}}\times\frac{1-\sqrt{1-[\delta_{cd}(x)]^2}}{\delta_{cd}(x)}\cos(\theta-\mathrm{j}) \tag{11}$$

This approximate inverse air-gap fluctuation is compared with the relatively precise inverse air-gap fluctuation at the initial position (i.e. θ = 0) in Figs. 3 (a), and Fig. 3 (b) shows the relative error of the approximate inverse air-gap function. It can be seen that the maximum error is less than 3%. Compared with the relative error mentioned in [8], this is also can be accepted when calculating the inductances of a SCIM with curved DE.

3. Inductances of a SCIM with Curved DE

According to winding function theory, the mutual inductance between any two windings *A* and *B* can be computed by [5, 8]

$$L_{AB}(\theta)=\mu_0 l_s\int_0^{2\pi} r_a(\varphi,\theta)g^{-1}(\varphi,\theta)\cdot n_A(\varphi,\theta)N_B(\varphi,\theta)d\varphi \tag{12}$$

where μ_0 is the permeability in vacuum, l_s is the axial stack length, $n_A(\varphi, \theta)$ is the turns function (winding distribution) of winding *A*, and $N_B(\varphi, \theta)$ is the winding function (magnetomotive force distribution along the air gap for a unit current flowing in the winding) of winding *B*. This method assumes no symmetry in the air-gap length or winding layout. All space harmonics of the winding magnetomotive force and the effect of eccentricity can be taken into account.

Due to the axial unequal air gap, the original WFA should be extended to 3-D to calculate the inductances in a SCIM with curved DE. Therefore, the differential mutual inductance of winding *A* and winding *B* is given as

$$dL_{AB}(x,\theta)=\mu_0\left[\int_0^{2\pi} r_a(x,\mathrm{j},\theta)g_{cd}^{-1}(x,\mathrm{j},\theta)\times n_A(\mathrm{j},\theta)N_B(\mathrm{j},\theta)d\mathrm{j}\right]dx \tag{13}$$

where the average air-gap radius $r_a(x, \varphi, \theta)$ is defined by

$$r_a(x,\varphi,\theta)=\frac{r_{i1}+r_{o2}(x,\varphi,\theta)}{2} \tag{14}$$

Similarly, it can be described by the expression:

$$r_a(x,\varphi,\theta)=r_0\left[1+\delta_{cd}(x)\cos(\theta-\varphi)\right] \tag{15}$$

where r_0 is the average radius of the air gap in a symmetrical SCIM. The equivalent inductance for the whole machine can be derived by

$$L_{AB}(\theta)=\int_0^{l_s} dL_{AB}(x,\theta) \tag{16}$$

Thus,

$$L_{AB}(\theta)=\mu_0\int_0^{l_s}\int_0^{2\pi} r_a(x,\mathrm{j},\theta)g_{cd}^{-1}(x,\mathrm{j},\theta)\times n_A(\mathrm{j},\theta)N_B(\mathrm{j},\theta)d\mathrm{j}dx \tag{17}$$

And the mutual inductance $L_{BA}(\theta)$ is given by

$$L_{BA}(\theta)=\mu_0\int_0^{l_s}\int_0^{2\pi} r_a(x,\mathrm{j},\theta)g_{cd}^{-1}(x,\mathrm{j},\theta)\times n_B(\mathrm{j},\theta)N_A(\mathrm{j},\theta)d\mathrm{j}dx \tag{18}$$

The self inductance of winding *A* also can be calculated by Eq. (17) with the subscript "*B*" replaced by "*A*".

4. Calculation of Inductances

The required inductances in the multi-loop model of a SCIM include the stator self and mutual inductances, rotor self and mutual inductances, and the mutual inductances between stator phases and rotor loops. Since the inductances of a SCIM under curved DE condition and pure DE condition are similar to some degree, a comparison is made between the calculation results under these two conditions in this section.

The specific machine studied in this paper is a three-phase four-pole star-connected 1200-kW squirrel-cage submersible induction motor. Fig. 4 shows the structure of the studied machine, and the detailed information of the machine is given in Table 1. Fig. 5 presents the turns functions and the winding functions of stator phase *a* and rotor loop 1. N_s represents the number of conductors per

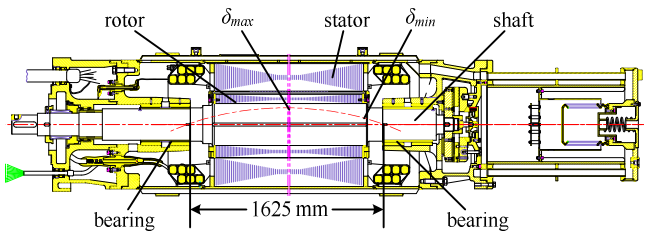

Fig. 4. Structure of the studied three-phase submersible induction motor

Table 1. Specifications of the proposed SCIM

Rated power (kW)	1200
Rated voltage (V)	6000
Winding connection	Y
Rated frequency (Hz)	50
Number of poles	4
Number of stator slots	36
Number of rotor bars	42
Air-gap length (mm)	2.0
Mean air-gap radius (mm)	174.0
Stack length (mm)	1400.0
Winding layers	1
Number of conductors per slot	12

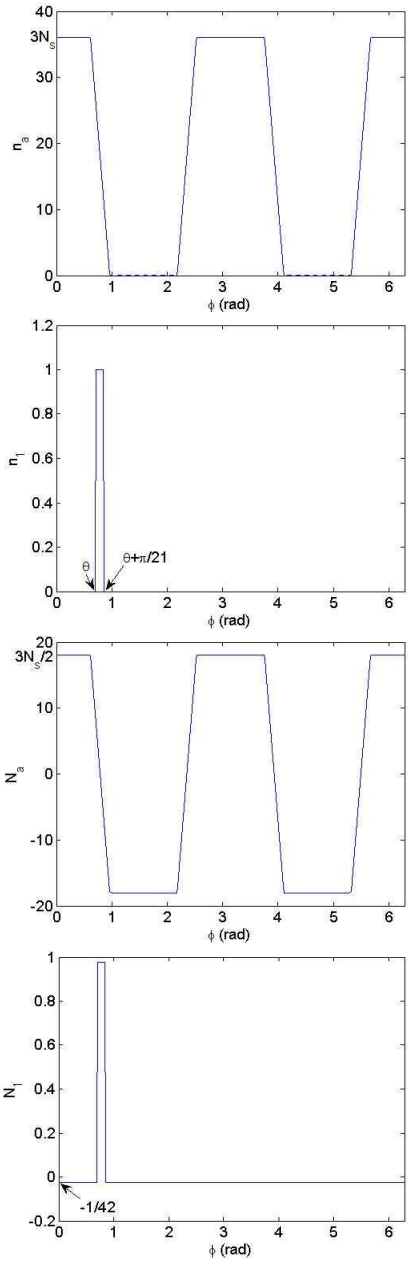

Fig. 5. Turns functions n (top) and winding functions N (bottom) of stator phase a (left) and rotor loop 1 (right)

Table 2. Studied curved DE conditions

	Level of curved DE		δ_{max}-δ_{min}	δ_{rms}
	δ_{min}	δ_{max}		
1	0.06	0.25	0.19	0.1961
2	0.10	0.40	0.30	0.3138
3	0.14	0.55	0.41	0.4314
4	0.18	0.70	0.52	0.5491
5	0.22	0.85	0.63	0.6668

slot. Clearly, the functions of stator phases are only about φ, and the functions of rotor loops are about both φ and θ. In order to investigate the inductance in its entirety, the calculation results under different levels of curved DE conditions are given in the paper. Table 2 lists several levels of curved DE conditions including the minimum eccentricity δ_{min}, maximum eccentricity δ_{max}, their difference, and the root mean square eccentricity. Fig. 5 illustrates the variations of $\delta_{cd}(x)$ under these levels of curved DE conditions. These curves are calculated based on the structure shown in Fig. 4.

The root mean square eccentricity is defined by $\delta_{rms} = \sqrt{\frac{1}{l_s}\int_0^{l_s}\left[\delta_{cd}(x)\right]^2 dx}$.

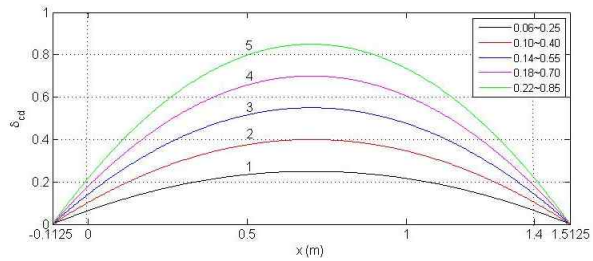

Fig. 6. Variations of the degrees of eccentricity under different levels of curved DE conditions

4.1 Stator self and mutual inductances

In the case of curved DE, the self inductances of the stator phases and the mutual inductances between stator phases are functions of rotor position θ because of the rotating position of the minimum air gap. Replacing the term $N_B(\varphi, \theta)$ with $N_A(\varphi, \theta)$, the stator self inductances also can be derived by (17). Fig. 7 shows the calculation results of self inductances of stator phase a (L_{aa}) and mutual inductances between stator phase a and b (L_{ab}) under different levels of curved DE conditions and pure DE conditions. Mutual inductance between stator phase a and c is not given because the amplitude equals to that of L_{ab}, and the phase is shifted to the left by $2\pi/3$. The constant values of stator inductances in a symmetrical machine are calculated as well: $L_{aa} = 0.2654$ H, $L_{ab} = L_{ac} = -0.1039$ H. Apparently, the existence of DE enlarges the magnitudes of stator self and mutual inductances. It is noted that the variations of stator inductances under curved DE conditions have much in common with that under pure

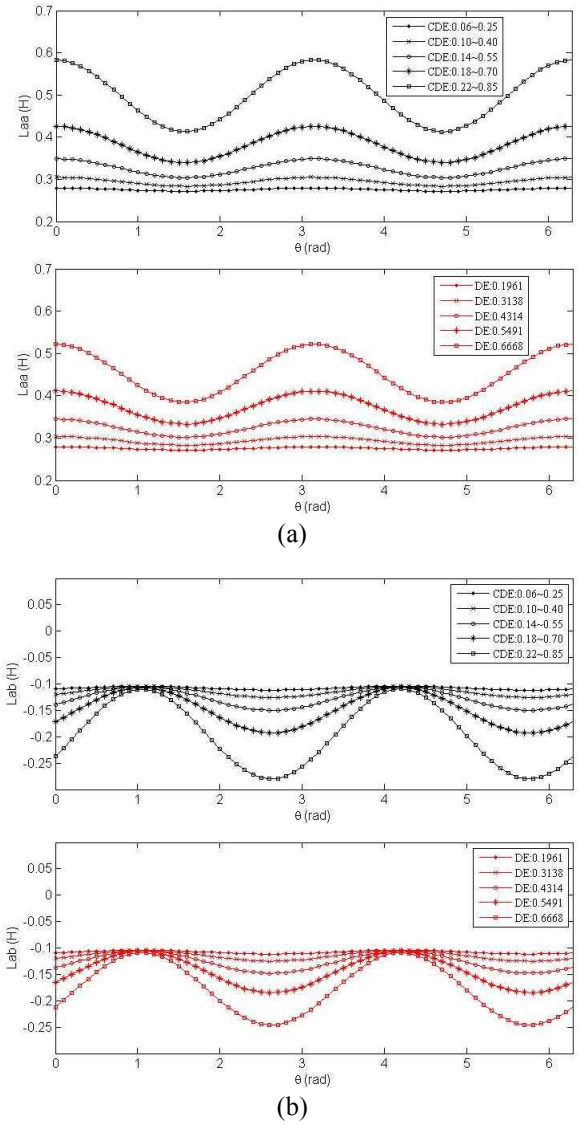

(a) (b)

Fig. 7. (a) Self inductances of stator phase *a* under curved DE conditions (top) and pure DE conditions (bottom). (b) Mutual inductances between stator phase *a* and *b* under curved DE conditions (top) and pure DE conditions (bottom)

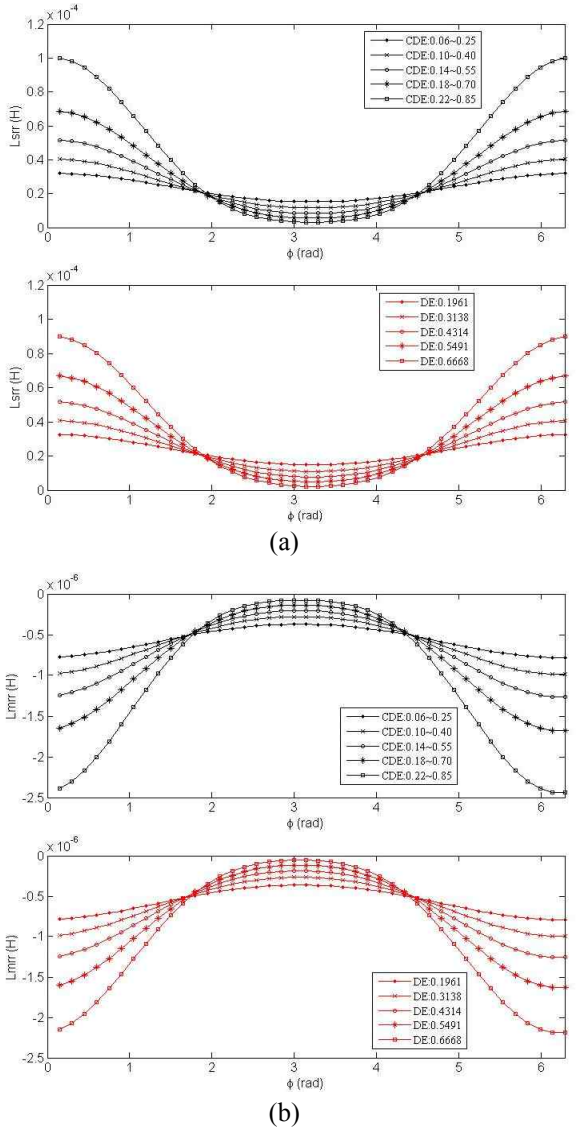

(a) (b)

Fig. 8. (a) Self inductances of rotor loops under curved DE conditions (top) and pure DE conditions (bottom). (b) Mutual inductances between rotor loop 1 and other loops under curved DE conditions (top) and pure DE conditions (bottom)

DE conditions. The calculation results get closer with the levels of curved DE and pure DE decline. Furthermore, it is easy to infer that there is a certain level of pure DE condition under which the variation of the inductance comes quite close to that under curved DE condition. And the certain level of pure DE must be between the minimum and maximum eccentricity of the corresponding curved DE. This point of view also can be applied to the inductances described in 4.2 and 4.3.

4.2 Rotor self and mutual inductances

Just like pure DE condition, rotor loops in curved DE case do not experience any change in air-gap length due to the rotating position of the minimum air gap. As a result, the self and mutual inductances of rotor loops are independent of rotor position θ, and all of the inductances can be computed only once. The rotor self and mutual inductances in a symmetrical machine are $L_{srr} = 2.235\times10^{-5}$ H, $L_{mrr} = -5.452\times10^{-7}$ H. Fig. 8 presents the rotor self and mutual inductances under different levels of curved DE conditions and pure DE conditions at initial position (as Fig. 2 shows). Clearly, the self inductance of the rotor loop located at the minimum air gap ($\varphi = 0$ or 2π) reaches the peak value. The value of mutual inductance declines with the rise of the distance between two rotor loops.

4.3 Mutual Inductances between Stator and Rotor

Stator phase-rotor loop mutual inductances are also

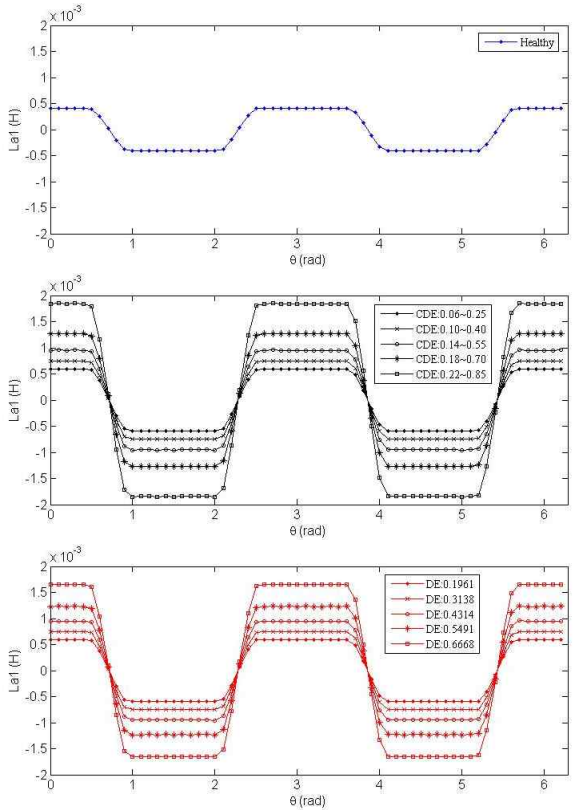

Fig. 9. Mutual inductances of stator phase *a* and rotor loop 1 under healthy (top), curved DE (middle), and pure DE (bottom) conditions

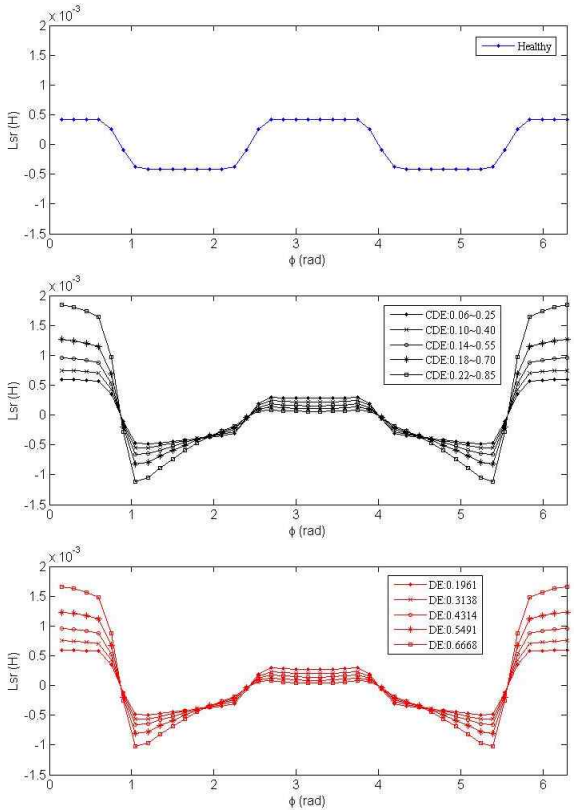

Fig. 10. Mutual inductances of stator phase *a* and rotor loops at the initial position under healthy (top), curved DE (middle), and pure DE (bottom) conditions

dependent on the rotor position θ. Fig. 9 shows the mutual inductances of the stator phase *a* and rotor loop 1 with respect to the rotor position under different levels of curved DE and pure DE conditions. The amplitude of inductance curve increases with the rise of the level of eccentricity. The mutual inductance between the stator phase *b* (or *c*) and rotor loop 1 is similar, just shifted by $2\pi/3$ (or $4\pi/3$) to the left. Fig. 10 presents the mutual inductances of the stator phase *a* and rotor loops at the initial position under different conditions. It can be seen that the amplitude of the mutual inductance increases with the decline of the air-gap length. In other words, the amplitude of mutual inductance between stator phase and rotor loop which located at the smaller air gap is greater than that between stator phase and rotor loop which located at the larger air gap.

However, it should be emphasized that the mutual inductances between rotor loops and stator phases are not equal to the mutual inductances between stator phases and rotor loops.

5. Conclusion

This paper presents a more accurate model of DE named as curved DE, and evaluates the inductances of a three-phase SCIM under curved DE condition using WFA. These inductances are used for dynamic simulation of electrical machines with DE or some other faults. It has been shown that there is a certain level of pure DE condition under which the inductance curves are nearly the same with those under the corresponding curved DE condition. In addition, the certain level of pure DE condition must be among the minimum and maximum eccentricity of the corresponding curved DE condition. That is to say, the dynamic simulation results, such as stator currents, of a machine with pure DE and another machine with curved DE will be quite similar. Yet, air gap eccentricity, if exists, in a large electrical machine is always somewhat curved in fact. So the actual eccentricity condition will be more terrible than the monitored eccentricity based on the conventional pure DE model. Further study is to incorporate the effect of SE (pure SE and inclined SE) as well as stator and rotor slots.

Acknowledgements

This work was supported by the National Natural Science Funds of China for Distinguished Young Scholar (No. 50925727), the National Natural Science Funds of China (No. 51177033 and No. 51377039), and Hefei Hengda Jianghai Pump Co; Ltd.

References

[1] A. Rezig, M. R. Mekideche, and Abdesslem, "Impact of eccentricity and demagnetization faults on magnetic noise generation in brushless permanent magnet DC motors," *Journal of Electrical Engineering & Technology*, vol. 6, no. 3, pp. 356-363, 2011.

[2] J. Faiz, B. M. Ebrahimi, B. Akin, and H. A. Toliyat, "Comprehensive eccentricity faults diagnosis in induction motors using finite element method," *IEEE Transactions on Magnetics*, vol. 45, no. 3, pp. 1764-1767, Mar. 2009.

[3] T. A. Lipo, "Analysis and control of synchronous machines," Course Notes for ECE 511, Department of Electrical and Computer Engineering, University of Wisconsin, Madison, 1986.

[4] X. Luo, Y. Liao, H. A. Toliyat, A. EI-Antably, and T. A. Lipo, "Multiple coupled circuit modeling of induction machines," *IEEE Transactions on Industry Applications*, vol. 31, no. 2, pp. 311-318. Mar./Apr. 1995.

[5] H. A. Toliyat, M. S. Arefeen, and A. G. Parlos, "A method for dynamic simulation of air-gap eccentricity in induction machines," *IEEE Transactions on Industry Applications*, vol. 32, no. 4, pp. 910-918, Jul./Aug. 1996.

[6] G. M. Joksimović, M. D. Đurović, J. Penman, and N. Arthur, "Dynamic simulation of dynamic eccentricity in induction machines - winding function approach," *IEEE Transactions on Energy Conversion*, vol. 15, no. 2, pp. 143-148, Jun. 2000.

[7] S. Nandi, R. M. Bharadwaj, and H. A. Toliyat, "Performance analysis of a three-phase induction motor under mixed eccentricity condition," *IEEE Transactions on Energy Conversion*, vol. 17, no. 3, pp. 392-399, Sep. 2002.

[8] J. Faiz, I. T. Ardekanei, and H. A. Toliyat, "An evaluation of inductances of a squirrel-cage induction motor under mixed eccentric conditions," *IEEE Transactions on Energy Conversion*, vol. 18, no. 2, pp. 252-258, Jun. 2003.

[9] J. Faiz, M. Ojaghi, "Stator inductance fluctuation of induction motor as an eccentricity fault index," *IEEE Transactions on magnetics*, vol. 47, no. 6, pp. 1775-1785, Jun. 2011.

[10] X. Li, Q. Wu, and S. Nandi, "Performance analysis of a three-phase induction machine with inclined static eccentricity," *IEEE Transactions on Industry Applications*, vol. 43, no. 2, pp. 531-541, Mar./Apr. 2007.

[11] A. Tenhunen, T. Benedetti, T. P. Holopainen, and A. Arkkio, "Electromagnetic forces in cage induction motors with rotor eccentricity," *IEEE International Conference on Electric Machines and Drives*, vol. 3, pp. 1616-1622, 2003.

[12] H. M. Kelk, A. Eghbali, and H. A. Toliyat, "Modeling and analysis of cage induction motors under rotor misalignment and air gap eccentricity," in *Conf. Rec.2005 IEEE International Conference on Industry Applications*, vol. 2, pp. 1324-1328.

[13] D. G. Dorrell, "Sources and characteristics of unbalanced magnetic pull in three-phase cage induction motors with axial-varying rotor eccentricity," *IEEE Transactions on Industry Applications.* vol. 47, no. 1, pp. 12-24, Jan. / Feb. 2011.

[14] D. G. Dorrell, "Calculation of unbalanced magnetic pull in small cage induction motors with skewed rotors and dynamic rotor eccentricity," *IEEE Transactions on Energy Conversion*, vol. 11, no. 3, pp. 483-488, Sep. 1996.

[15] D. G. Dorrell, W. T. Thomson, and S. Roach, "Analysis of airgap flux, current, and vibration signals as a function of the combination of static and dynamic airgap eccentricity in 3-phase induction motors," *IEEE Transactions on Industry Applications*, vol. 33, no. 1, pp. 24-34, Jan./Feb. 1997.

[16] S. Nandi, S. Ahmed, and H. A. Toliyat, "Detection of rotor slot and other eccentricity related harmonics in a three phase induction motor with different rotor cages," *IEEE Transactions on Energy Conversion*, vol. 14, no. 3, pp. 253-260, Sep. 2001.

Qiang Lv He received the B.S. degree in 2011 in electrical engineering from Hefei University of Technology, Hefei, China. He joined the School of Electrical Engineering and Automation, Hefei University of Technology as a postgraduate. His main research interests are in the field of motor design, and finite element analysis.

Xiaohua Bao He received the B.S. degree in 1996, the M.Sc. degree in 2002 and the Ph.D. degree in 2008, all in electrical engineering from Hefei University of Technology, Hefei, China. He joined the School of Electrical Engineering and Automation, Hefei University of Technology and was promoted to Professor, in 2012. He was a visiting Scholar with Virginia Polytechnic Institute and State University, U.S. His main research interests are in the field of motor design, magnetic field analysis, and finite element analysis.

Yigang He He received the M.Sc. degree in electrical engineering from Hunan University, Changsha, China, in 1992 and the Ph.D. degree in electrical engineering from Xi'an Jiaotong University, Xi'an, China, in 1996. In 1990, he joined the College of Electrical and Information Engineering, Hunan University and was promoted to Associate Professor, Professor in 1996, 1999, respectively. From 2006 to 2011, he worked as the director of the Institute of Testing Technology for Circuits and Systems, Hunan University. He was a Senior Visiting Scholar with the University of Hertfordshire, Hatfield, U.K., in 2002. In 2011, he joined the Hefei University of Technology, China, and currently works as the Head of School of Electrical and Automation Engineering, Hefei University of Technology. His teaching and research interests are in the areas of circuit theory and its applications, testing and fault diagnosis of analog and mixed-signal circuits, electrical signal detection, motor measuring technology, analysis & calculation of electrical motor & electromagnetic fields, smart grid, radio frequency identification technology, and intelligent signal processing. He has published some 200 journal and conference papers in the aforementioned areas and several chapters in edited books. Dr. He has been on the Technical Program Committees of a number of international conferences. He was the recipient of a number of national and international awards, prizes, and honors.

Yong Fang He received the B.S. degree in 2012 in electrical engineering from Hefei University of Technology, Hefei, China. He joined the School of Electrical Engineering and Automation, Hefei University of Technology as a postgraduate. His main research interests are in the field of motor design, and electromagnetic field analysis.

Xiaowei Cheng He received the B.S. degree in 2011 in physics from Shangqiu Normal University, Henan, China. He joined the School of Electrical Engineering and Automation, Hefei University of Technology as a postgraduate. His main research interests are in the field of motor design, and motor insulation research.